Hindawi
Advances in Materials Science and Engineering
Volume 2019, Article ID 9723763, 15 pages
https://doi.org/10.1155/2019/9723763

Research Article

Tea Stem as a Sorbent for Removal of Methylene Blue from Aqueous Phase

Tzan-Chain Lee,[1] Shumao Wang,[1,2] Zonggui Huang,[1] Zhongxing Mo,[1] Gangxing Wang,[1] Zhuanrong Wu,[1] Chengshun Liu,[1] Hua Han,[1] and Tzu-Hsing Ko[1]

[1]*Anxi College of Tea Science, Fujian Agriculture and Forestry University, Fuzhou city, Fujian Province, China*
[2]*Institute of Tea Science, Zhejiang University, Hangzhou city, Zhejiang Province, China*

Correspondence should be addressed to Tzu-Hsing Ko; hsingko@gmail.com

Received 16 April 2019; Revised 20 July 2019; Accepted 28 July 2019; Published 22 September 2019

Academic Editor: Yee-wen Yen

The potentiality of tea stem for the adsorption of methylene blue (MB) from aqueous phase was investigated. A series of operating factors, including the initial MB concentration, contact time, pH of solution, dose of tea stem, and ionic strength of solution, were conducted to understand the effect of adsorption of MB onto tea stem. Adsorption isotherm, kinetic models, thermodynamic investigation, and regenerability of tea stem were systematically investigated in this study. The experiment results revealed that the removal efficiency decreased with MB concentration and the equilibrium time of adsorption at different initial MB concentrations was approximately at 60 min. The appropriate dose of tea stem powder was found to be 4 g/L. The pH_{zpc} of tea stem was evaluated and was observed to be 6.0 ± 0.2. The removal efficiency increased with pH ranging from 3.0 to 5.0 and remained constantly at the pH range of 5.0–11.0. The pH affected the adsorption because of the repellent power between H^+ and dye cation. The ionic strength was found to have a negligible effect on the adsorption. The Langmuir and Temkin isotherm models were found to be the best isotherm models to elucidate the adsorption mechanism between MB and tea stem powder. The maximum adsorption capacity of 103.09 mg/g derived from the Langmuir model was much close to the experimental result. From the kinetic analysis, the pseudo-second-order model was found to be the suitable model to describe the adsorption behavior. The calculated adsorption capacities at different temperatures derived from the pseudo-second-order model ranging from 68.91 to 69.8 mg/g were well close to the experimental data. The intraparticle diffusion of MB molecules into pore structures of tea stem powder is the rate-limiting step for the adsorption process in this study. Evaluation of thermodynamic parameters including changes in enthalpy, entropy, and Gibb's free energy indicated the adsorption mechanism between MB and tea stem powder was a spontaneous and exothermic process. The regeneration/adsorption experiments indicated that the tea stem powder efficiently remained more than 97% after five cycles using NaOH as a desorbing agent and thus be used for many times. On the basis of experimental results obtained, it is concluded that the tea stem has a considerable potential as a low-cost sorbent for removing MB from the aqueous phase.

1. Introduction

Dyes are widely applied in many fields such as textile, leather tanning industries, paper production, food technology, and medical treatment, which has propelled the development of technology and industry in recent years [1–4]. However, untreated wastewater is discharged into the environment, thereby causing river and soil pollution [5, 6]. Because of the variety, high chromaticity, refractory degradation, and poor biodegradability of dyes, this pollution has exceeded the limit in the environment and affected human health [6–9]. Solving the dye-induced pollution problem is increasingly crucial. Current methods to dyestuff wastewater treatment include coagulation, advanced oxidation, membrane separation, biodegradation, and adsorption [10–14], all of which were limited to apply in industries because of more chemical consumption, complex operating conditions, and second pollution [15–18]. Adsorption, however, has advantages such as low cost, environmental safety, regeneration, and easy operational feasibility when compared with other

methods, which attracts people to explore new approaches to solve the dyestuff wastewater problem [6, 7, 19]. Methylene blue (MB) is extensively used as a chemical indicator, biological stain, disinfectant, and medicine in water bodies such as lakes, dyeing of tissues, and treating methemoglobinemia, respectively [19, 20]. Many materials such as halloysite/$MnFe_2O_4$ nanocomposites, kaolin, and palygorskite/carbon composite have been widely used to adsorb MB [21, 22]. In addition, the experiments were systematically conducted using kinetic, isotherm, and thermodynamic models to determine the possible adsorption mechanism.

Tea, cultivated in countries from China to Kenya, is a vital plant and well-known nonalcoholic drink globally. It is a kind of biosorption material with a net-like structure and highly developed pore structure. After drinking, tea residue is discarded as waste. However, some studies have proven that tea waste exhibits better adsorption performance for heavy metal removal and dye removal [23–26]. Recently, researches have reported that MB can be absorbed by many materials and tea has a great potential as an adsorbent. Oolong tea is one of the important tea beverages in China. Tea stem is a by-product from the manufacture of oolong tea. In the past, many tea stems are discarded during the manufacture of oolong tea because of low reuse. Undoubtedly, most of the wasted tea stems have been largely produced in China, leading to a severe environmental problem. To our knowledge, the use of tea stem on the removal of dye-pollutants from aqueous solution is not reported. The main objective of this study was to evaluate the potential of tea stem as an alternative adsorbent for the removal of MB from aqueous solution. A series of operative factors, including contact time, initial MB concentration, dose of tea stem, pH value, and ionic strength on the removal efficiency was experimentally investigated. The equilibrium isotherms were determined by several models to understand the mechanism of MB. Furthermore, the kinetics involved in the adsorption process was evaluated at different temperatures.

2. Materials and Methods

2.1. Preparation of Tea Stem Powder. Tea stem separated from Tieguanyin species was collected from the local tea market, Anxi County, Fujian Province. Five hundred grams of tea stem were mixed with 2 L of distilled water and then were brewed at 373 K for 4 hrs, and the operation was repeated at least 6 times. The brewed solution was detected by a UV-visible spectrophotometer to confirm that the signal of brewed solution was close to the background value (absorbance signal less than 0.01). After brewing, tea stem samples were dried at 383 K for 12 hrs. The dry tea stem samples were crushed to pass through an 80-mesh sieve for obtaining the desired particle sizes. The prepared tea stem powders were stored in a dry container for the adsorption experiment. Through the elemental analysis, the content of carbon, nitrogen, and hydrogen for tea stem used in this study was 48.06%, 1.35%, and 0.41%. The water content and ash content were 4.85% and 0.80%, respectively.

2.2. Analytical Instrument and Chemical Reagents. The MB concentration was analyzed using a UV-visible spectrophotometer (Shimadzu Model UV 1750) at a wavelength of 664 nm. The calibration curve was obtained by using the standard of MB reagent, and the correlation coefficient R^2 was determined more than 0.995 to ensure the accuracy.

The surface area was measured with a Micromeritics ASAP 2010 instrument using adsorption of nitrogen at 77 K. Prior to adsorption measurements, the samples were degassed under a vacuum of 5 μm Hg at 373 K for 2 hrs.

Fourier transform infrared spectroscopy was used to identify the surface functional groups of tea stem powder. The infrared spectra were recorded on a Perkin-Elmer One B model FTIR spectrometer with fully computerized data storage and data handing capability. To provide adequate characterization of the wasted tea powder, the spectrum was set from a range of 400 to 4,000 cm^{-1}. A 100-scan data accumulation was carried out at 4 cm^{-1} resolution.

Elementar vario EL III Heraeus CHNOS Rapid F002, equipped with a flash combustion furnace and thermal conductivity detector (TCD), was used for determination the content of carbon and nitrogen in tea stem.

2.3. Batch Studies. The concentration of MB used for the experiments of pH values, dose of tea stem, and ionic strength was controlled at 300 mg/L. The ratio of tea stem weight and MB solution volume (labelled as RM) was used, and the ranges of 2–40 g/L were investigated in this study for determining the effect of dose of tea stem on adsorption of MB. The pH value of the MB solution was adjusted to the desired value by adding a small quantity of HCl and NaOH to investigate the effect of pH on adsorption. The concentrations of MB with different pH values were measured, and the results indicated that there are no appreciable changes in the signal of UV-visible spectra of MB in the used pH range. The pH value at different concentrations of MB was measured between 4.9 and 5.1, showing a stable pH range for the adsorption experiment. All adsorption experiments were carried in conical flask with a 50 mL of MB solution and were placed on a thermocontrolled shaker at 200 rpm. After adsorption experiment, the solution was centrifuged at 5000 rpm for 10 mins, and then the supernatant solution was analyzed to determine the concentration of MB. The adsorption capacity (mg/g) and removal efficiency (%) of MB were calculated using the following equations:

$$Q_t = \frac{C_0 - C_t}{M} \times V,$$
$$E = \frac{C_0 - C_t}{C_0} \times 100, \quad (1)$$

where C_0 and C_t are the concentrations under the phase of liquid at the initial time and any time t in mg/L, respectively. Q_t is the amount of MB uptake at any time t in mg/g. V is the volume of the solution in liters and M is the mass of tea stem powder in gram. All adsorption experiments were performed in duplicate, and the data were further analyzed.

2.4. Investigation Point of Zero Charge (pH_{zpc}) of Tea Stem Powder. For better understanding the effect of pH in

adsorption of MB onto tea stem powder, pH_{zpc} assay of tea stem powder was tested according to the report of Ali et al. [15]. A volume of 50 mL NaCl (0.01 mol/L) solution was added in flask as an electrolyte. A solution with initial pH value ranging from 3.0 to 10.0 was prepared and 4 g/L of tea stem were added in different initial pH solutions. The mixed solution was shaken at an agitation speed of 200 rpm for 12 hrs at 298 K. After shaking, tea stem powder was filtered and the final pH value was determined.

2.5. Adsorption Kinetics. Adsorption kinetic experiments were operated at different temperatures (298, 313, and 328 K) with a MB concentration of 300 mg/L and a certain mass of 0.2 g tea stem powder. Different kinetic models were applied to fit the adsorption process in this study.

The pseudo-first-order model was established by *Lagergren*. The linear form of the model is expressed as follows [27]:

$$\log\left(Q_e - Q_t\right) = \log Q_e - \left(\frac{k_1}{2.303}\right)t, \tag{2}$$

where Q_e and Q_t represent the adsorption capacity (mg/g) at equilibrium and any time t, respectively. k_1 (min^{-1}) is the rate constant that is related to the adsorption equilibrium rate. The plot of the pseudo-first-order model is from log (Q_e–Q_t) versus t.

The pseudo-second-order model originated from Wu et al. [28]. The model is expressed as follows:

$$\frac{t}{Q_t} = \frac{1}{k_2 Q_e^2} + \frac{t}{Q_e}, \tag{3}$$

where Q_e and Q_t represent the adsorption capacity (mg/g) at equilibrium and any time t, respectively. k_2 (min^{-1}) is the rate constant related to the adsorption equilibrium rate.

The Elovich model was developed by Siddiqui et al.[29, 30]. The linearized form is expressed as follows:

$$Q_t = \frac{1}{\beta}\ln(\alpha\beta) + \frac{1}{\beta}\ln t, \tag{4}$$

where Q_t (mg/g) represents the adsorption capacity at any time t, β is the coefficient representing rate of desorption, and α is the initial rate coefficient for the adsorption and also represents the activation energy for the chemical adsorption. α and β can be calculated from intercept and slope of the plot between Q_t versus ln t.

Bangham model was contrived by Bangham [31, 32]. The linearized form is expressed as follows:

$$\log\log\left(\frac{C_0}{C_0 - Q_t m}\right) = \log\left(\frac{k_3 m}{2.303V}\right) + \alpha\log t, \tag{5}$$

where C_0 (mg/L) is the initial concentration of the solution, Q_t (mg/g) represents the adsorption capacity at any time t, m (g/L) and V (L) are the mass of adsorbent and volume of the solution, and k_3 and α are constants. $\log\log(C_0/C_0 - Q_t m)$ and $\log t$ make up the plot, where k_3 and α can be determined from the slope and intercept.

To ascertain the specific adsorption mechanism for adsorption of MB onto tea stem powder, the intraparticle-diffusion model was used to further analyze the results. According to the intraparticle-diffusion model, the adsorption process is divided three stages [33]: (i) dye molecules gather in the film of liquid outside the adsorbent, (ii) dye molecules enter into the pores onto the adsorbent, and (iii) dye molecules are adsorbed by the active positions inner pores onto adsorbents and reach equilibrium. The intraparticle-diffusion model is given as follows [34]:

$$q = K_{id}\sqrt{t} + C, \tag{6}$$

where K_{id} is the rate constant involved in the intraparticle-diffusion model in $mg\,g^{-1}\,min^{-0.5}$, and C is the constant related to the thickness of the boundary layer. If the linearized plot passes through the origin, then the adsorption rate is only controlled by internal diffusion; if not, both the external diffusion and internal diffusion dominantly control the adsorption rate, and the higher the values of C, the greater the external diffusion effect produced [33, 34].

2.6. Isotherm Models. The Langmuir isotherm model establishes that adsorption occurs on active sites of the sorbent with equivalent energy, and a monolayer of the adsorbate exists on the solid homogeneous surface [35]. The model is expressed as follows:

$$\frac{C_e}{Q_e} = \frac{C_e}{Q_m} + \frac{1}{Q_m b}, \tag{7}$$

where C_e and Q_e are the MB concentration (mg/L) and the amount of MB adsorbed at equilibrium state (mg/g), respectively, Q_m is the maximum amount of the monolayer of MB occurring on the homogeneous solid surface (mg/g), and b is the Langmuir constant (L/mg). Both Q_m and b are calculated from the slope and intercept of the plots of C_e/Q_e versus C_e. The constant b was calculated from the intercept of the plot that was further determined a dimensionless separation factor, R_L. R_L confirms the characteristic of the Langmuir isotherm model, especially the type of isotherm. The R_L model is expressed as follows [36]:

$$R_L = \frac{1}{1 + bC_0}, \tag{8}$$

where C_0 is the initial MB concentration, and if $R_L > 1$, then the adsorption process could be unfavorable; if $1 > R_L > 0$, the adsorption process could be energetically favorable; if $R_L = 1$, then the adsorption process could be linear; and if $R_L = 0$, the adsorption process is irreversible.

The Freundlich isotherm model, an empirical model, is used to describe that the adsorbates are adsorbed to heterogeneous surfaces of a multilayer adsorption system [37, 38]. The model can be expressed as follows:

$$\log Q_e = \log K_f + \frac{1}{n}\log C_e, \tag{9}$$

where K_f and n are the rate constants related to the adsorption capacity (mg/g) and adsorption intensity and their values were obtained from the intercept and slope of the plots of Q_e against C_e. In this model, adsorption process is favorable if $1/n$ is closer to zero, whereas the adsorption is

unfavorable if $1/n$ is larger than one. The adsorption is homogeneous, and no reaction occurs between the adsorbent and adsorbate when $1/n$ is one [39, 40].

Temkin isotherm model, taking interaction between adsorbate and adsorbent into account, assumes that (i) the heat of sorption linearly decreases with the increasing of surface coverage and (ii) bonding energies are equally distributed on the adsorbent. The linearized model is given as follows [27, 41, 42]:

$$Q_e = \frac{RT}{b} \ln C_e + \frac{RT}{b} \ln A, \tag{10}$$

where R is gas constant (8.314 J/mol/K) and T is the absolute temperature, and A and b are the Temkin constants that are related to maximum bonding energies (L/mg) and the heat of sorption (J/mol), respectively. They are determined from the slope and intercept of the plot of Q_e against ln C_e.

Dubinin–Radushkevich (D-R) isotherm model is applied to definite the nature of bonding happened on the heterogeneous. The linearized model is given as follows [27, 29, 43]:

$$\ln Q_e = \ln Q_{D-R} - \beta\varepsilon^2, \tag{11}$$

where Q_e and $Q_{D\text{-}R}$ are the amount of MB adsorbed at equilibrium state (mg/g) and the theoretical uptake of tea stem powder (mg/g). ε is Polanyi potential, which can be computed by the model:

$$\varepsilon = RT \ln\left(1 + \frac{1}{C_e}\right), \tag{12}$$

where R is gas constant ($8.314 * 10^{-3}$ kJ/mol/K) and T is the absolute temperature, C_e is the concentration of MB (mg/L) when adsorption process achieving equilibrium state, β is related to the mean free energy E (kJ/mol) of adsorption per mole of MB. E can be calculated by following model:

$$E = \frac{1}{\sqrt{2\beta}}. \tag{13}$$

E value is used to evaluate physisorption or chemisorption; when E value is less than 8 kJ/mol, the adsorption is physisorption, and when E value is 8–16 kJ/mol, the adsorption is chemisorption.

2.7. Adsorption Thermodynamics. To understand the thermodynamic parameters, the Gibbs free energy, enthalpy, and entropy were considered and experiments were conducted at 298, 313, and 328 K with a 300 mg/L of MB solution. The models of thermodynamic parameters are expressed as follows [44, 45]:

$$\ln k = \frac{\Delta S^0}{R} - \frac{\Delta H^0}{RT}, \tag{14}$$

where k is the rate constant related to adsorption under the equilibrium state. ΔS^0 and ΔH^0 are the standard entropy change in J/mol K and the standard enthalpy change in kJ mol, respectively. T is the absolute temperature (K), and R is the gas constant (8.314 J/mol K). ΔS^0 and ΔH^0 are determined from the slope and intercept, respectively, of the plot of ln k against $1/T$. The standard Gibbs free energy of adsorption (ΔG^0) is expressed as follows:

$$\Delta G^0 = -RT \ln k. \tag{15}$$

2.8. Regeneration and Reusability. For the regeneration process, the used tea stem powder was regenerated by mixing of 0.05 N NaOH solutions at a shaker for 60 min at 298 K. The used tea powder was separated from the suspension and washed with deionized water in ultrasonic shaker for 60 min and repeated for three times. After ultrasonic treatment, the regenerated tea stem was dried in an oven at 333 K.

3. Results and Discussion

3.1. Pore Structure and Surface Characteristic of Tea Stem. The N_2 adsorption and desorption isotherms of tea stem powder are shown in Figure 1. A detectable hysteresis loop is observed between $P/P_0 = 0.9 - 1.0$. This confirms that the isotherm curve corresponds to the characteristic of type IV according to the classification standard of International Union of Pure and Applied Chemistry, suggesting the major pore structure may be in the form of a cylindrical or silt shape [46]. The BET surface area of tea stem powder was measured to be 1.05 m^2/g. The pore size calculated using BJH method was 18.95 nm. The feature of hysteresis loop was suggested to be related to the capillary condensation associated with large pore channel. Thus, the pores on tea stem powder were macropores, mesopores, and micropores, of which the mesopores were major. XRD patterns showed that the width peaks at $2\theta = 25.5$ and $2\theta = 34.6$ were observed and assigned to the cellulose and lignin, respectively. FTIR analysis revealed that the bonded-OH groups (3416 cm^{-1}), aliphatic C-H group (2925 cm^{-1}), C=O stretching (1650 cm^{-1}), C-H bending (1385 cm^{-1}), C-O-C of polysaccharides (1150 cm^{-1}), and C-O-H stretching (1062 cm^{-1}) were the main functional groups on the surface of tea stem.

3.2. Effect of Initial MB Concentration and Contact Time. Figure 2 shows the adsorption capacity and removal efficiency as a function of contact time at different MB concentrations. As shown, a rapid adsorption stage is observed in the initial contact time, which is followed by a stable adsorption stage. The adsorption capacity increases from 24.25 to 99.44 mg/g when the initial MB concentration increases from 100 to 800 mg/L. This is due to that the driving force established in the high initial concentration may have surmounted the obstruction of MB adsorption between the liquid and solid phases [47, 48]. In addition, the high MB concentration enhances the collisional frequency between MB and tea stem powder and thus increases the adsorption process [48]. The removal efficiency decreases with the initial MB concentration, which is attributed to the finite adsorption sites on the surface of tea stem powder. The equilibrium time for adsorption at different initial MB concentrations is approximately at 60 min. With time

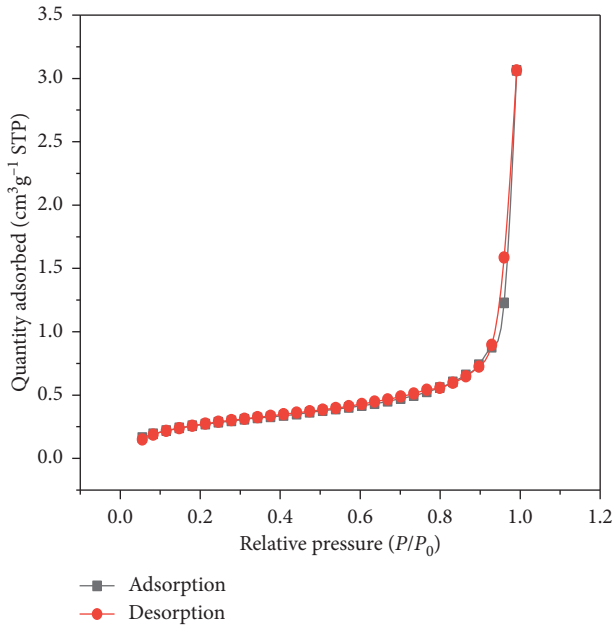

Figure 1: N_2 adsorption and desorption isotherms of tea stem powder used in this study.

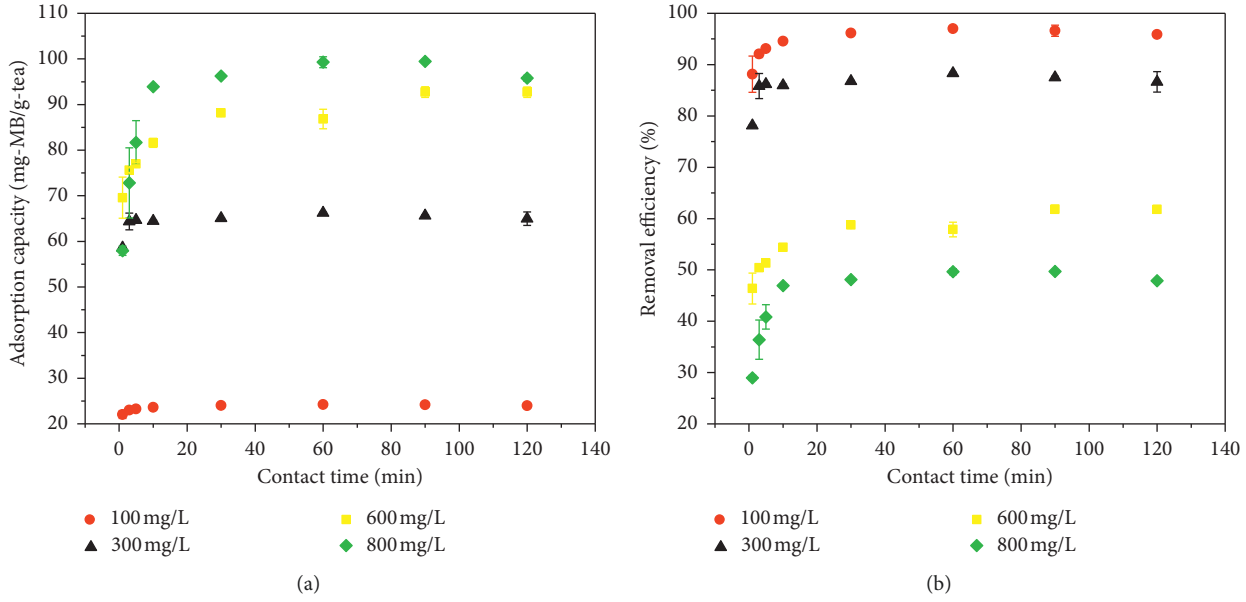

Figure 2: Effect of the contact time and initial MB concentration on the adsorption of MB: (a) adsorption capacity; (b) removal efficiency (RM = 4 g/L; temp. = 298 K; pH = 5.00).

increase, the adsorption of MB stabilized, indicating that the adsorption sites saturated [49].

3.3. Effect of the Dose of Tea Stem Powder. Figure 3 depicts the adsorption capacity and removal efficiency for different doses of tea stem powder ranging from 2 to 40 g/L. The adsorption reaches an equilibrium state when the contact time is at 60 min. The adsorption capacity decreases from 121.47 to 7.47 mg/g, and the removal efficiency increases from 80.98 to 99.50% as the contact time is progressed from 1 to 120 min. This is attributed to the amorphous and porous structures of tea stem powder and available active adsorption sites that increase with the strength of the dose of tea stem powder, and thus, decrease in driving force [29]. Based on the experimental results in this study, the appropriate dose of tea stem powder was 4 g/L because more than 90% of removal efficiency and an acceptable adsorption capacity were achieved.

3.4. Effect of pH. The pH and pH_{zpc} are important factors for adsorption of MB onto tea stem powder. The change in

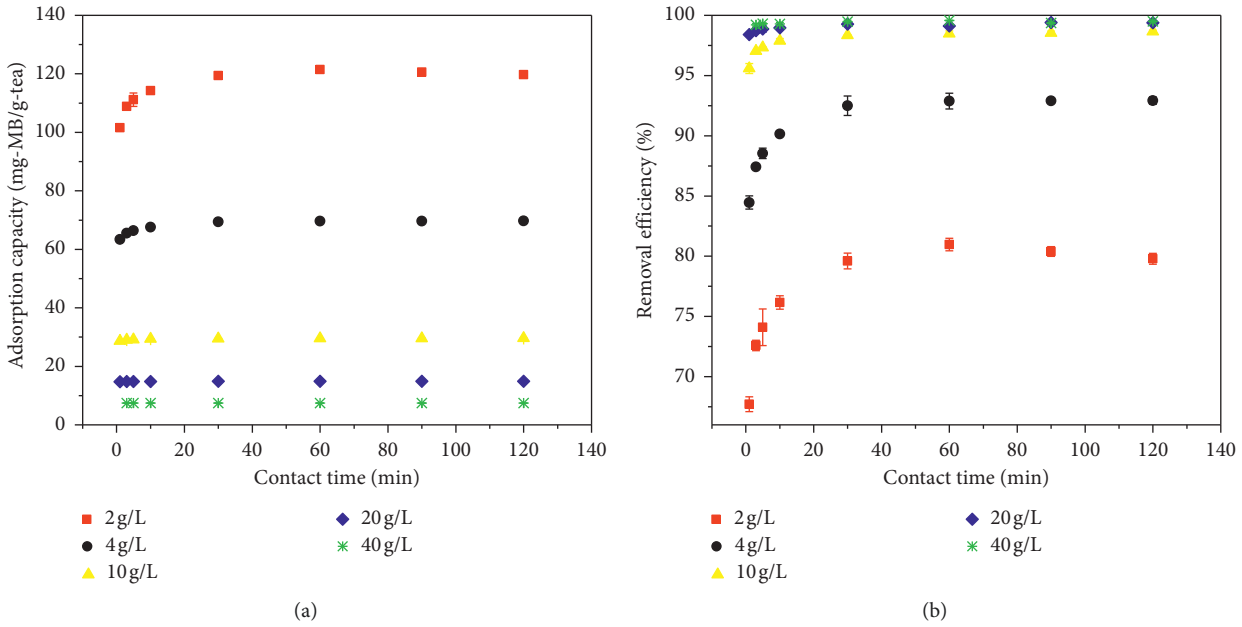

Figure 3: Effect of doses of tea stem powder on the adsorption of MB: (a) adsorption capacity; (b) removal efficiency ($C = 300$ mg/L; temp. = 298 K; pH = 5.00).

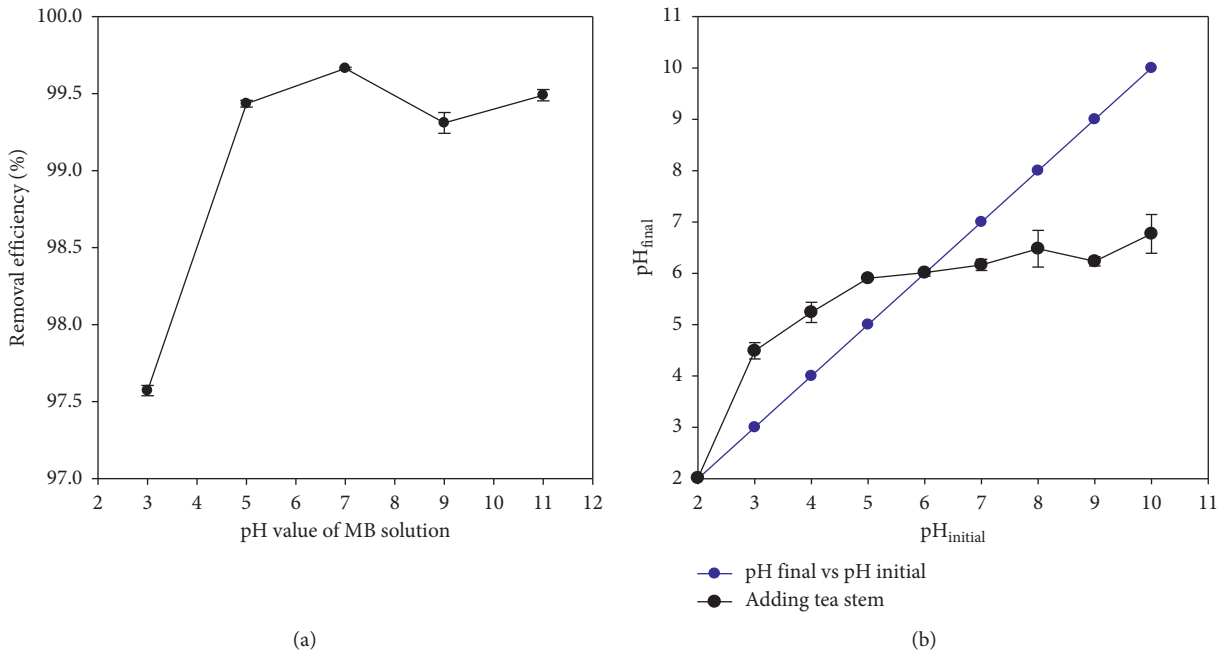

Figure 4: (a) Effect of pH of MB solution on the removal efficiency and (b) the point of zero charge for tea stem ($C = 300$ mg/L; RM = 4 g/L; temp. = 298 K; time = 60 min).

pH_{zpc} provides the charge characteristic of tea stem and determines the type of charge when pH is changed in the experimental process. Figure 4 shows the effect of pH on the adsorption of MB and the graph of $pH_{initial}$ versus pH_{final}. The removal efficiency increases from 97.57 to 99.44% as pH increases from 3.00 to 5.00. With the pH increases from 5.00 to 11.00, the removal efficiency is more than 99.00% and remains constantly. The pH_{zpc} is estimated about 6.00 ± 0.2 and the surface charges are toward to the negatively charged when pH is greater than 6.0, whereas when the pH is lower than 6.0, the tea stem surface becomes positively charged. MB is a cationic dye and possesses positively charged ions in aqueous solution. Under the lower pH condition, the concentration of H^+ ion is high, causing a competition for active sites of MB between H^+ ion and cationic groups on MB. Therefore, the adsorption efficiency of MB declines. On the other hand, higher positive charge of the MB solution and simultaneous protonation of tea stem powder at low pH

cause a decrease in available adsorption sites. The electrostatic interaction between the positively charged MB and H^+ weakens the adsorption process. Conversely, occurrence of deprotonation of the tea stem powder increases the number of active adsorption sites and reduces electrostatic force [29, 50, 51]. Therefore, the effect of pH on the adsorption of MB in this study reveals that the removal efficiency maintains constantly at the pH range of 5.0–11.0, which agrees with the pH_{zpc} of tea stem powder.

3.5. Effect of Ionic Strength. In addition to dye, wastewater also contains large amount of inorganic salt. For a better understanding of its effect on adsorption efficiency, a series of different NaCl concentrations were investigated. Figure 5 illustrates the adsorption capacity and removal efficiency at different concentrations of NaCl. The adsorption capacity and removal efficiency decreases from 23.35 to 22.96 mg/g, and 93.40 to 91.86%, respectively, as NaCl increases from 2.00 to 8.00%. Slight decreases in adsorption capacity and removal efficiency prove that the ionic strength may be negligible on the adsorption of MB onto tea stem powder. Furthermore, the affinitive interaction between dye molecules and tea stem powder is stronger than that between Na^+ and tea stem powder.

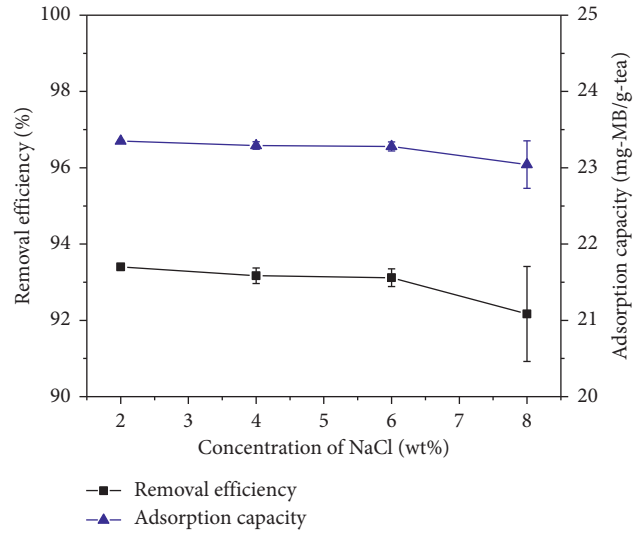

FIGURE 5: Effect of ionic strength on the removal efficiency and adsorption capacity of MB (C = 100 mg/L; RM = 4 g/L; temp. = 298 K; time = 60 min; pH = 5.00).

3.6. Study of Kinetic

3.6.1. Pseudo-First-Order and Second-Order Models. The fitting results of the pseudo first-order and second-order models at different temperatures are shown in Figure 6, and the detailed kinetic parameters are listed in Table 1. The R^2 values for the pseudo-first-order are ranged between 0.49 and 0.84 at different temperatures, while the values of R^2 for the second-order are more than 0.99. The predictive maximum adsorption capacities (Q_{cal}) for the pseudo-first-order and second-order models are estimated to be 3.22, 6.45, and 1.98 mg/g and 69.93, 69.44, and 69.49 mg/g at different temperatures, respectively. The Q_{cal} values derived from pseudo-second-order are much close to the experimental values (Q_{exp}), demonstrating that the pseudo-second-order model is more appropriate for the prediction of kinetic process for MB adsorption onto tea stem powder. The idea fitting of the pseudo-second-order model means that the rate-limiting step is not the resistance of boundary layer and the adsorption of MB onto tea stem is a complicated process [52].

3.6.2. Elovich Model. The results of the Elovich model are shown in Figure 6(c) and Table 1. The R^2 values for the Elovich model are 0.95, 0.93, and 0.72 at 298, 313, and 328 K, respectively, showing the Elovich model could describe the adsorption of MB onto tea stem powder at 298 and 313 K rather than at 328 K. Values of α and β are $1.05 * 10^{21}$, $3.51 * 10^{16}$, 0.75, and 0.61 at 298 K and 313 K, respectively. Note that α is absolutely higher than β, which indicates that the adsorption process is the main reaction. This also explained why the initial adsorption rate of MB onto tea stem powder was high and the adsorption rate decreased with contact time. In addition, the results of the Elovich model confirmed that adsorption of MB onto tea stem powder was chemisorption, which agreed with inferences of the pseudo-second-order model.

3.6.3. Bangham Model. The results of Bangham model are shown in Figure 6(d) and Table 1. The R^2 values for the Bangham model at 298, 328, and 313 K are 0.96, 0.96, and 0.76, respectively, which indicates that the film diffusion is the rate-controlling step at 298 and 313 K. As the temperature increases, R^2 value for Bangham model is smaller and proves that the film diffusion is not the rate-controlling step.

3.6.4. Intraparticle-Diffusion Model. As shown in Figure 6(e), three stages are observed from the multilinear plots. The first adsorption stage, with the highest values of K_{id}, could be controlled not only by intraparticle diffusion, but also by external diffusion to some extent because the origin was not passed. The first stage has a higher slope than the other stages. The resistance of mass transfer between the external boundary layer film of liquid and adsorbent is relatively smaller, resulting in the rapid adsorption rate for the first linear stage. Another reason may be due to the MB molecules accumulating outside the tea stem powder and the reaction among the MB cation and charges on the surfaces of tea stem powder. The second adsorption stage could be explained by that the MB molecules gradually penetrated the inner macropores and mesoporous in tea stem powder. The values of K_{id} of the third adsorption stage were small, which indicated that the adsorption reached the equilibrium state. The third adsorption stage was affected by the numbers of microspores, size of MB molecules, diffusion resistance, and the concentration of MB.

3.7. Study of Adsorption Isotherm

3.7.1. Langmuir Isotherm Model. The results of the Langmuir isotherm model are presented in Figure 7(a) and

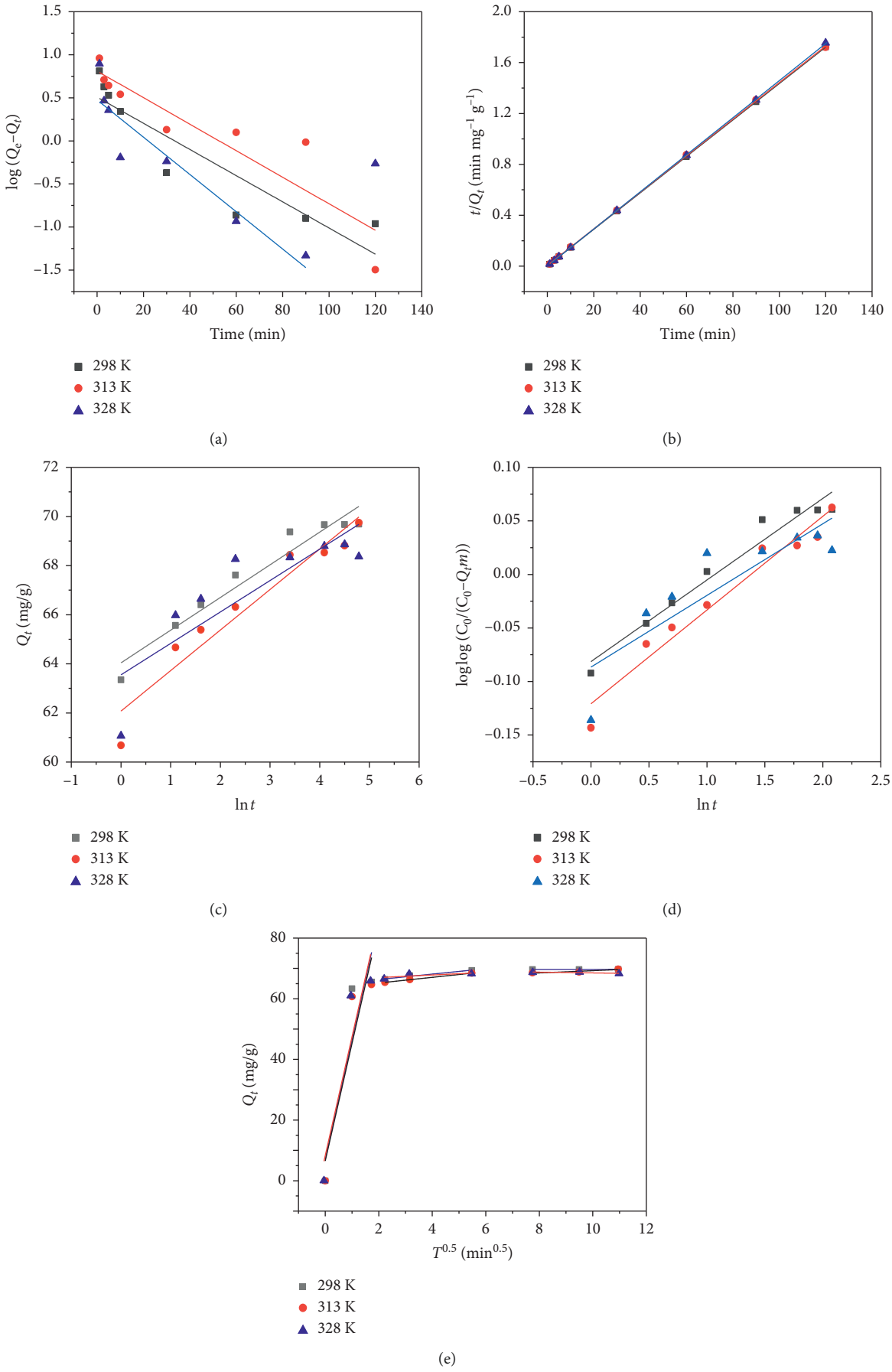

Figure 6: Fitting plots of (a) pseudo-first-order model, (b) pseudo-second-order model, (c) Elovich model, (d) Bangham model, and (e) intraparticle-diffusion model for the adsorption of MB onto tea stem powder (C = 300 mg/L; RM = 4 g/L; time = 60 min; pH = 5.00).

Table 1: Adsorption kinetic fitting results for the MB adsorption onto tea stem powder. ($C = 300$ mg/L; RM = 4 g/L; pH = 5.00).

Temperature (K)	Q_{exp} (mg/g)	Pseudo-first-order model			Pseudo-second-order model			Elovich model			Bangham model			Intraparticle diffusion model								
		k_1 (1/min)	R^2	Q_{cal} (mg/g)	k_2 (1/min)	R^2	Q_{cal} (mg/g)	α	β	R^2	α	k_3	R^2	K_{id} (first stage)	C	R^2	K_{id} (second stage)	C	R^2	K_{id} (third stage)	C	R^2
298	69.80	0.04	0.84	3.22	0.07	1.00	69.93	$1.05 * 10^{21}$	0.75	0.95	0.08	0.02	0.96	39.36	7.13	0.85	0.89	64.58	0.98	0.01	69.59	0.97
313	69.78	0.04	0.84	6.45	0.04	1.00	69.44	$3.51 * 10^{16}$	0.61	0.93	0.09	0.02	0.96	38.72	6.53	0.86	1.14	62.76	0.99	0.09	67.89	0.88
328	68.91	0.03	0.49	1.98	0.21	1.00	68.49	$4.66 * 10^{21}$	1.98	0.72	0.07	0.02	0.76	39.45	6.42	0.87	1.62	63.11	1.00	0.11	67.88	0.90

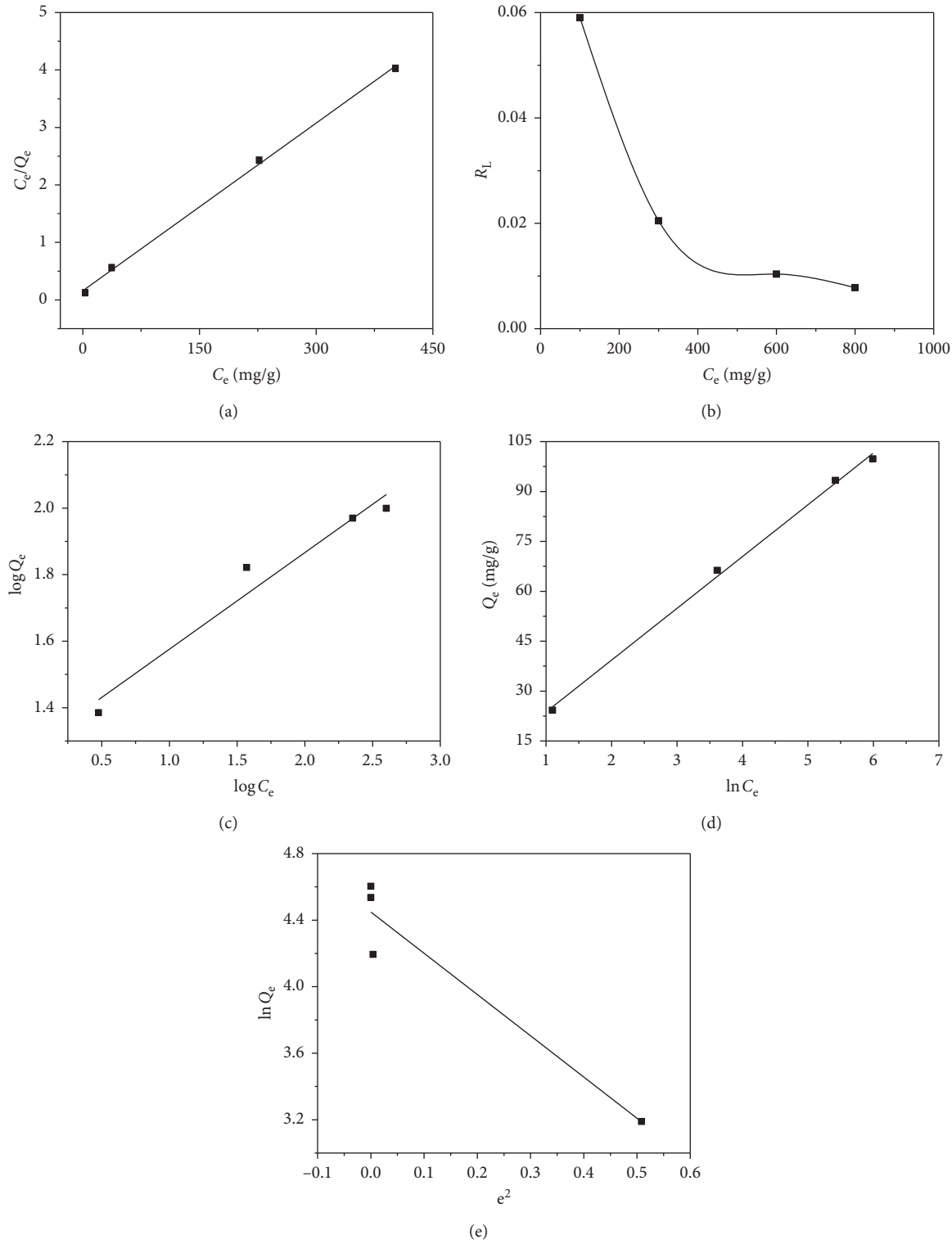

Figure 7: Adsorption isotherm plots for adsorption of MB onto tea stem powder: (a) Langmuir model, (b) RL distribution, (c) Freundlich model, (d) Temkin model, and (e) D-R model (RM = 4 g/L; temp. = 298 K; pH = 5.00).

Table 2. The R^2 value for Langmuir isotherm model was 0.99, which demonstrates the adsorption of MB onto tea stem powder is chemisorption with equivalent energy on the adsorption sites and monolayer of the MB on the tea stem powder. All values of R_L obtained from the Langmuir isotherm model are less than 1 and decreased with C_e (shown in Figure 7(b)). This result attests that the adsorption of MB onto tea stem powder is favorable. The monolayer coverage of MB onto wasted tea powder is the main adsorption mechanism.

Table 2: Adsorption isotherm fittings for the MB adsorption onto tea stem powder (RM = 4 g/L; pH = 5.00).

Temperature (K)	Q_{exp} (mg/g)	Langmuir			Freundlich			Temkin			D-R			
		Q_{max} (mg/g)	b (L/mg)	R^2	$1/n$	K_f (mg/g)	R^2	A (L/mg)	b (J/mol)	R^2	$Q_{D\text{-}R}$ (mg/g)	β	E (kJ/mol)	R^2
298	99.80	103.09	0.06	0.99	0.29	19.31	0.96	1.70	159.41	0.99	85.53	2.48	0.64	0.93

3.7.2. Freundlich Isotherm Model. Figure 7(c) shows the Freundlich isotherm model for adsorption of MB onto tea stem powder, and relevant isotherm parameters as well as correlation coefficients are presented in Table 2. The R^2 value for Freundlich isotherm model is 0.96, which is lower than that of the Langmuir isotherm model. The adsorption of MB onto tea stem powder is favorable because of lower $1/n$ value (0.29).

3.7.3. Temkin Isotherm Model. The Temkin isotherm model presented in Figure 7(d) and Table 2 also appears to have the better R^2 in this study. The value of A, bonding energy between MB molecules and tea stem powder is 1.70 L/mg, and equally distributes. In addition, the heat of adsorption (b value) is 159.41 J/mol, which linearly decreases as MB molecules covered gradually tea stem powder. These findings suggest that the electrostatic interaction is one of the important mechanisms between wasted tea powder and MB [52].

3.7.4. D-R Isotherm Model. The description of D-R isotherm model is shown in Figure 7(e) and Table 2. The $Q_{D\text{-}R}$ and β for adsorption of MB onto tea stem powder are 85.53 mg/g and 2.48, respectively. The R^2 value for D-R isotherm model is 0.93, which is the lowest among the isotherm models used in this study. Therefore, the D-R isotherm model probably is not suitable to elucidate the adsorption of MB onto tea stem powder.

3.8. Analysis of Thermodynamics. The relationship between ln K and $1/T$ and the calculated thermodynamic parameters are shown in Figure 8 and Table 3. The values of ΔG^0 are −6.49, −6.75, and −6.62 kJ/mol at 298, 313, and 328 K, respectively, which demonstrates that the adsorption process is spontaneous. The negative ΔH^0 (−5.18 kJ/mol) denotes that the exothermal reaction occurs between the MB and tea stem powder. The positive value of ΔS^0 (4.60 J/mol K) signifies the increase in disorder at the interface of MB and tea stem powder. The result of negative ΔH^0 and positive ΔS^0 agrees with the spontaneous adsorption process. More importantly, the analysis of thermodynamic studies is similar to that of adsorption isothermal and kinetic studies.

3.9. Regeneration Studies. Regeneration and recyclability of adsorbent is important to evaluate the overall performance of adsorbent in the practical application. To explore the regenerability of tea stem, a five regeneration/adsorption cycles was carried out and the result is shown in Figure 9. Note that the total iron content was estimated approximately 2.46 ± 0.12 mg/g-tea stem and its influence on regeneration can be neglected in this study. The excellent regeneration performance was found after regeneration. The removal efficiencies remain constantly (more than 97%) and no deactivation is observed, which denotes tea stem powder is a potential adsorbent for removing MB. The clear color of MB solution after five regeneration/adsorption cycles reveals that the tea stem is easily to be regenerated. The possible explanations for the excellent regeneration performance of tea stem can be attributed to the complete desorption of MB from the surface of tea stem powder when the NaOH was used as a desorbing agent. Additionally, the surface and pore structure of tea stem may be modified through the regeneration process, and the adsorption sites on tea stem powder are more active and are difficult to collapse and clog [53]. Based on the regeneration evaluation, it is deduced that the NaOH proves to be a desorbing agent and tea stem is an inexpensive, ecofriendly, and competent adsorbent for the remediation of dyes from aqueous system.

3.10. Comparison with Other Adsorbents. The comparison of maximum adsorption capacity of tea stem for MB with those of other adsorbents in the literature is shown in Table 4. The tea stem shows the comparable adsorption capacity for MB with respect to the adsorbents. Tea stem has a higher adsorption capacity among the adsorbents in Table 4. Therefore, tea stem is a suitable adsorbent for removal of MB.

4. Conclusion

Tea stem was used as a sorbent for the adsorption of MB from aqueous phase in a batch mode. The removal efficiency decreased as the initial concentration of MB increased because of the competition among dye cations. The adsorption process achieved equilibrium when the contact time was 60 min. According to the removal efficiency and adsorption capacity, the optimum dose of tea stem powder was 4 g/L. The pH_{zpc} of tea stem powder was found to be 6.00 ± 0.20, and the pH range of 5.0–7.0 would be the optimal condition for adsorption. The ionic strength was found to have a negligible effect on the adsorption.

From the kinetics and isotherm investigation, the pseudo-second-order model performed well at 298, 313, and 328 K, denoting the adsorption process of MB onto tea stem was multistage chemisorption. Analysis of Elovich and Bangham models illustrated that film diffusion was the rate-controlling step at 298 and 313 K. The well fitting for the pseudo-second-order model and Langmuir isotherm model revealed that the possible adsorption process was chemical, spontaneous, and monolayer adsorption. Temkin isotherm model suggested that the bonding energy between MB molecules and tea stem powder was 1.70 L/mg and equally

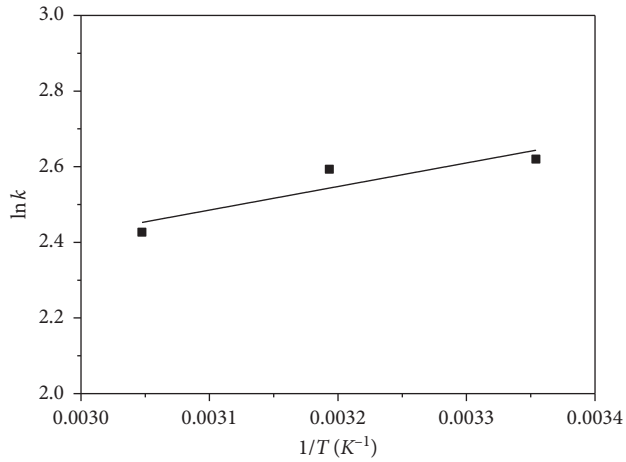

Figure 8: Plot of ln k versus $1/T$ for the adsorption of MB onto tea stem powder ($C = 300$ mg/L; RM = 4 g/L; time = 60 min; pH = 5.00).

Table 3: Thermodynamic parameters for MB adsorption onto tea stem powder ($C = 300$ mg/L; RM = 4.00 g/L; pH = 5.00).

Temperature (K)	ΔG^0 (kJ/mol)	ΔH^0 (kJ/mol)	ΔS^0 (J/mol/k)
298	−6.49		
313	−6.75	−5.18	4.60
328	−6.62		

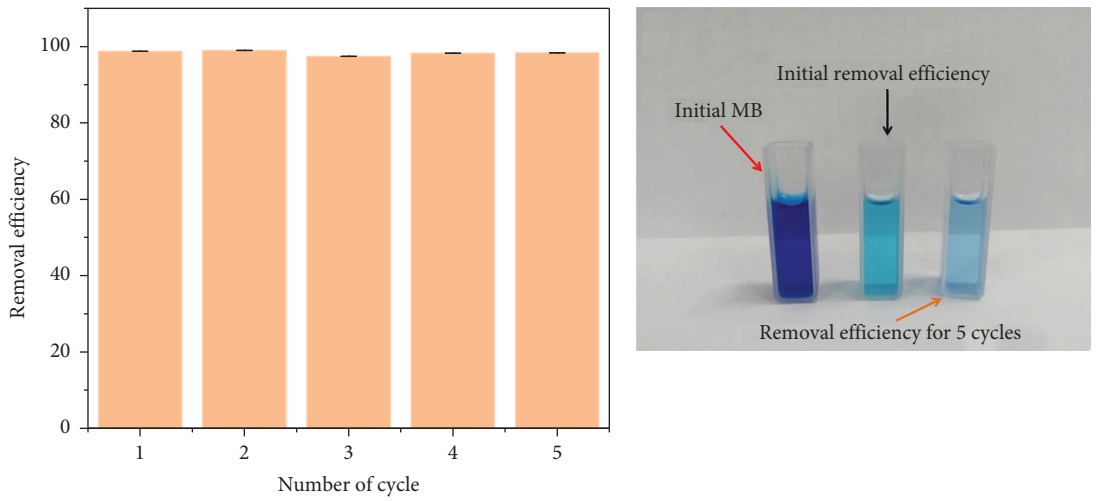

Figure 9: Regeneration of tea stem powder: (a) removal efficiency of MB adsorption for 5 cycles and (b) color of MB solutions before and after tea stem adsorption ($C = 300$ mg/L; RM = 4 g/L; temp. = 298 K; time = 60 min; pH = 5.00).

Table 4: Adsorption capacity of MB on different adsorbents.

Adsorbent	Adsorption capacity of MB (mg/g)	Reference
Raw algerian kaolin	52.76	[21]
Mesoporous silica	65.70	[54]
Rice husk	28.50	[55]
Hydrophilic silica aerogel	47.21	[56]
Acid washed black cumin seed	73.53	[57]
Wheat samples	46.00	[58]
Date palm leaves	58.10	[59]
Tea stem powder	103.09	This study

distributed on tea stem powder. The heat of sorption was 159.41 J/mol, which linearly decreased as MB molecules covered gradually tea stem powder. The initial adsorption stage was controlled by external diffusion and intraparticle diffusion, and the second adsorption stage was controlled by the rate-limiting step. Thermodynamic studies, especially the values of ΔG^0, ΔS^0, and ΔH^0, concurred with the analysis results of the kinetics and adsorption equilibrium studies. Thermodynamic investigation indicated the adsorption mechanism between MB and tea stem powder was a spontaneous and exothermic process. The regeneration/adsorption experiments indicated that the tea stem powder remained more than 97% efficiently after five cycles using NaOH as a desorbing agent and thus be used for many times. Although tea stem is a potential sorbent for the removal of MB and some operating factors and their effect were carried out in a batch experiment, other reactor systems, such as a fixed bed reactor or continuous stirred tank reactor (CSTR), should be thoroughly considered in the future. In addition, some other isotherm models including Redlich–Peterson isotherm (combination of Langmuir-Freundlich model), Sip model, Toth model, Koble–Corrigan model (three-parameters empirical model on the combination of the Langmuir and Freundlich) could be taken into account for a better understanding of the possible adsorption behavior. Briefly, as demonstrated in this study, tea stem powders have a huge potential as sorbents for removing dye pollution.

Data Availability

The data generated and analyzed in this manuscript are available from the correspondence author on reasonable request.

Conflicts of Interest

The authors declare that there are no conflicts of interest regarding the publication of this paper.

Authors' Contributions

T. C. Lee, S. Wang, and T. H. Ko conceived and designed the research and experiments. Z. Huang, Z. Mo, and G. Wang performed the experiments. Z. Wu, C. Liu, and H. Han collected data and performed the model analysis. T. C. Lee, S. Wang, and T. H. Ko wrote the paper. All authors have read and approved the final manuscript. Tzan-Chain Lee and Shumao Wang equally contributed to this work.

Acknowledgments

This work was partially funded by the construction of modern agricultural and industrial park for Anxi County, Fujian Province, Minister of Agriculture and Rural Affairs, China (KMD18003A).

References

[1] E. Forgacs, T. Cserháti, and G. Oros, "Removal of synthetic dyes from wastewaters: a review," *Environment International*, vol. 30, no. 7, pp. 953–971, 2004.

[2] M. Kaya, "Evaluation of a novel woody waste obtained from tea tree sawdust as an adsorbent for dye removal," *Wood Science and Technology*, vol. 52, no. 1, pp. 245–260, 2018.

[3] Y.-X. Chen, R.-C. Li, Y.-H. Zhang, X.-G. Chen, and Y. Ye, "Adsorption of methylene blue by halloysite/MnFe2O4 nanocomposites," *Journal of Nanoscience and Nanotechnology*, vol. 17, no. 9, pp. 6489–6496, 2017.

[4] M. Wainwright, "In defence of "dye therapy"," *International Journal of Antimicrobial Agents*, vol. 44, no. 1, pp. 26–29, 2014.

[5] C. D. Raman and S. Kanmani, "Textile dye degradation using nano zero valent iron: a review," *Journal of Environmental Management*, vol. 177, pp. 341–355, 2016.

[6] R. Koswojo, R. P. Utomo, Y.-H. Ju et al., "Acid green 25 removal from wastewater by organo-bentonite from Pacitan," *Applied Clay Science*, vol. 48, no. 1-2, pp. 81–86, 2010.

[7] H. Kono, K. Ogasawara, R. Kusumoto, K. Oshima, H. Hashimoto, and Y. Shimizu, "Cationic cellulose hydrogels cross-linked by poly(ethylene glycol): preparation, molecular dynamics, and adsorption of anionic dyes," *Carbohydrate Polymers*, vol. 152, pp. 170–180, 2016.

[8] C. Singh, A. Goyal, and S. Singhal, "Nickel-doped cobalt ferrite nanoparticles: efficient catalysts for the reduction of nitroaromatic compounds and photo-oxidative degradation of toxic dyes," *Nanoscale*, vol. 6, no. 14, pp. 7959–7970, 2014.

[9] J. B. Joo, J. Park, and J. Yi, "Preparation of polyelectrolyte-functionalized mesoporous silicas for the selective adsorption of anionic dye in an aqueous solution," *Journal of Hazardous Materials*, vol. 168, no. 1, pp. 102–107, 2009.

[10] Y.-Y. Lau, Y.-S. Wong, T.-T. Teng, N. Morad, M. Rafatullah, and S.-A. Ong, "Degradation of cationic and anionic dyes in coagulation-flocculation process using bi-functionalized silica hybrid with aluminum-ferric as auxiliary agent," *RSC Advances*, vol. 5, no. 43, pp. 34206–34215, 2015.

[11] A. Zuorro and R. Lavecchia, "Evaluation of UV/H_2O_2 advanced oxidation process (AOP) for the degradation of diazo dye reactive green 19 in aqueous solution," *Desalination and Water Treatment*, vol. 52, no. 7–9, pp. 1571–1577, 2014.

[12] D. Daâssi, S. Rodríguez-Couto, M. Nasri, and T. Mechichi, "Biodegradation of textile dyes by immobilized laccase from coriolopsis gallica into Ca-alginate beads," *International Biodeterioration & Biodegradation*, vol. 90, pp. 71–78, 2014.

[13] X.-F. Sun, S.-G. Wang, W. Cheng et al., "Enhancement of acidic dye biosorption capacity on poly(ethylenimine) grafted anaerobic granular sludge," *Journal of Hazardous Materials*, vol. 189, no. 1-2, pp. 27–33, 2011.

[14] Y. C. Xu, Z. X. Wang, X. Q. Cheng, Y. C. Xiao, and L. Shao, "Positively charged nanofiltration membranes via economically mussel-substance-simulated co-deposition for textile wastewater treatment," *Chemical Engineering Journal*, vol. 303, pp. 555–564, 2016.

[15] A. B. Ali, K. Babak, R. Mohammad et al., "Comparative treatment of textile wastewater by adsorption, Fenton, UV-Fenton and US-Fenton using magnetic nanoparticles -functionalized carbon (MNPs@C)," *Journal of Industrial and Engineering Chemistry*, vol. 56, pp. 163–174, 2017.

[16] M. Ahmadi, M. H. Niari, and B. Kakavandi, "Development of maghemite nanoparticles supported on crosslinked chitosan (γ-Fe_2O_3@CS) as a recoverable mesoporous magnetic composite for effective heavy metals removal," *Journal of Molecular Liquids*, vol. 248, pp. 184–196, 2017.

[17] A. A. Isari, A. Payan, M. Fattahi, S. Jorfi, and B. Kakavandi, "Photocatalytic degradation of rhodamine B and real textile wastewater using Fe-Doped TiO_2 anchored on reduced graphene oxide (Fe-TiO_2/rGO): characterization and feasibility,

mechanism and pathway studies," *Applied Surface Science*, vol. 462, pp. 549–564, 2018.

[18] B. Kakavandi, A. Takdastan, S. Pourfadakari, M. Ahmadmoazzam, and S. Jorfi, "Heterogeneous catalytic degradation of organic compounds using nanoscale zero-valent iron supported on kaolinite: mechanism, kinetic and feasibility studies," *Journal of the Taiwan Institute of Chemical Engineers*, vol. 96, pp. 329–340, 2019.

[19] D. Tucker, Y. Lu, and Q. Zhang, "From mitochondrial function to neuroprotection-an emerging role for methylene blue," *Molecular Neurobiology*, vol. 55, no. 6, pp. 5137–5153, 2018.

[20] M. S. Cooper, M. Randall, M. Rowell, M. Charlton, A. Greenway, and C. Barnes, "Congenital methemoglobinemia type II-clinical improvement with short-term methylene blue treatment," *Pediatric Blood & Cancer*, vol. 63, no. 3, pp. 558–560, 2016.

[21] L. Mouni, L. Belkhiri, J.-C. Bollinger et al., "Removal of methylene blue from aqueous solutions by adsorption on kaolin: kinetic and equilibrium studies," *Applied Clay Science*, vol. 153, pp. 38–45, 2018.

[22] X.-P. Wu, Y.-Q. Xu, X.-L. Zhang, Y.-C. Wu, and P. Gao, "Adsorption of low-concentration methylene blue onto a palygorskite/carbon composite," *New Carbon Materials*, vol. 30, no. 1, pp. 71–78, 2015.

[23] I.-S. Ng, X. Wu, X. Yang, Y. Xie, Y. Lu, and C. Chen, "Synergistic effect of *Trichoderma reesei* cellulases on agricultural tea waste for adsorption of heavy metal Cr(VI)," *Bioresource Technology*, vol. 145, pp. 297–301, 2013.

[24] C.-H. Weng, Y.-T. Lin, D.-Y. Hong, Y. C. Sharma, S.-C. Chen, and K. Tripathi, "Effective removal of copper ions from aqueous solution using base treated black tea waste," *Ecological Engineering*, vol. 67, pp. 127–133, 2014.

[25] A. A. Babaei, A. Khataee, E. Ahmadpour, M. Sheydaei, B. Kakavandi, and Z. Alaee, "Optimization of cationic dye adsorption on activated spent tea: equilibrium, kinetics, thermodynamic and artificial neural network modeling," *Korean Journal of Chemical Engineering*, vol. 33, no. 4, pp. 1352–1361, 2016.

[26] R. J. Khan, A. N. S. Saqib, R. Farooq, R. Khan, and M. Siddique, "Removal of Congo red from aqueous solutions by spent black tea as adsorbent," *Journal of Water Chemistry and Technology*, vol. 40, no. 4, pp. 206–212, 2018.

[27] S. A. Chaudhry, T. A. Khan, and I. Ali, "Adsorptive removal of Pb(II) and Zn(II) from water onto manganese oxide-coated sand: isotherm, thermodynamic and kinetic studies," *Egyptian Journal of Basic and Applied Sciences*, vol. 3, no. 3, pp. 287–300, 2016.

[28] Z. Wu, X. Yuan, H. Zhong et al., "Enhanced adsorptive removal of p-nitrophenol from water by aluminum metal-organic framework/reduced graphene oxide composite," *Scientific Reports*, vol. 6, no. 1, p. 25638, 2016.

[29] S. I. Siddiqui, G. Rathi, and S. A. Chaudhry, "Acid washed black cumin seed powder preparation for adsorption of methylene blue dye from aqueous solution: thermodynamic, kinetic and isotherm studies," *Journal of Molecular Liquids*, vol. 264, pp. 275–284, 2018.

[30] M. Ahmadi, M. Foladivanda, N. Jaafarzadeh et al., "Synthesis of chitosan zero-valent iron nanoparticles supported for cadmium removal: characterization, optimization and modeling approach," *Journal of Water Supply: Research and Technology—Aqua*, vol. 66, no. 2, pp. 116–130, 2017.

[31] V. S. Mane, I. D. Mall, and V. C. Srivastava, "Kinetic and equilibrium isotherm studies for the adsorptive removal of brilliant green dye from aqueous solution by rice husk ash," *Journal of Environmental Management*, vol. 84, no. 4, pp. 390–400, 2007.

[32] W. O. Abdel, "Kinetic and isotherm studies of copper (II) removal from wastewater using various adsorbents," *Egyptian Journal of Aquatic Research*, vol. 33, no. 1, pp. 125–143, 2007.

[33] L. Tang, L. Li, R. Chen, C. Wang, W. Ma, and X. Ma, "Adsorption of acetone and isopropanol on organic acid modified activated carbons," *Journal of Environmental Chemical Engineering*, vol. 4, no. 2, pp. 2045–2051, 2016.

[34] B. H. Hameed and M. I. El-Khaiary, "Batch removal of malachite green from aqueous solutions by adsorption on oil palm trunk fibre: equilibrium isotherms and kinetic studies," *Journal of Hazardous Materials*, vol. 154, no. 1–3, pp. 237–244, 2008.

[35] M. V. Subbaiah and Y. S. Yun, "Biosorption of Nickel(II) from aqueous solution by the fungal mat of *Trametes versicolor* (rainbow) biomass: equilibrium, kinetics, and thermodynamic studies," *Biotechnology and Bioprocess Engineering*, vol. 18, no. 2, pp. 280–288, 2013.

[36] H. Liu, L. Chen, and J. Ding, "Adsorption behavior of magnetic amino-functionalized metal-organic framework for cationic and anionic dyes from aqueous solution," *RSC Advances*, vol. 6, no. 54, pp. 48884–48895, 2016.

[37] A. Ahmad, A. H. Bhat, and A. Buang, "Biosorption of transition metals by freely suspended and Ca-alginate immobilised with *Chlorella vulgaris*: kinetic and equilibrium modeling," *Journal of Cleaner Production*, vol. 171, pp. 1361–1375, 2018.

[38] V. K. Gupta, A. Rastogi, and A. Nayak, "Biosorption of nickel onto treated alga (*Oedogonium hatei*): application of isotherm and kinetic models," *Journal of Colloid and Interface Science*, vol. 342, no. 2, pp. 533–539, 2010.

[39] A. Alshameri, H. He, J. Zhu et al., "Adsorption of ammonium by different natural clay minerals: characterization, kinetics and adsorption isotherms," *Applied Clay Science*, vol. 159, pp. 83–93, 2018.

[40] N. Bordoloi, R. Goswami, M. Kumar, and R. Kataki, "Biosorption of Co (II) from aqueous solution using algal biochar: kinetics and isotherm studies," *Bioresource Technology*, vol. 244, pp. 1465–1469, 2017.

[41] D. Vuono, E. Catizzone, A. Aloise et al., "Modelling of adsorption of textile dyes over multi-walled carbon nanotubes: equilibrium and kinetic," *Chinese Journal of Chemical Engineering*, vol. 25, no. 4, pp. 523–532, 2017.

[42] B. Kakavandi, A. Raofi, S. M. Peyghambarzadeh, B. Ramavandi, M. H. Niri, and M. Ahmadi, "Efficient adsorption of cobalt on chemical modified activated carbon: characterization, optimization and modeling studies," *Desalination and Water Treatment*, vol. 111, pp. 310–321, 2018.

[43] X. Tao, Y. Wu, and H. Sha, "Cuprous oxide-modified diatomite waste from the brewery used as an effective adsorbent for removal of organic dye: adsorption performance, kinetics and mechanism studies," *Water, Air, & Soil Pollution*, vol. 229, no. 10, pp. 1–19, 2018.

[44] T. Şahan, F. Erol, and Ş. Yılmaz, "Mercury (II) adsorption by a novel adsorbent mercapto-modified bentonite using ICP-OES and use of response surface methodology for optimization," *Microchemical Journal*, vol. 138, pp. 360–368, 2018.

[45] Z.-F. Yang, L.-Y. Li, C.-T. Hsieh, R.-S. Juang, and Y. A. Gandomi, "Fabrication of magnetic iron oxide@graphene composites for adsorption of copper ions from aqueous solutions," *Materials Chemistry and Physics*, vol. 219, pp. 30–39, 2018.

[46] Y.-Q. Zhao, H.-L. Zhao, Y.-H. Liang, Q.-Y. Jia, and B.-B. Zhang, "Preparation and characterization of CuO-CoO-MnO/SiO2 nanocomposite aerogels as catalyst carriers," *Transactions of Nonferrous Metals Society of China*, vol. 20, no. 8, pp. 1463–1469, 2010.

[47] A. Ozer, G. Akkaya, and M. Turabik, "The removal of acid red 274 from wastewater: combined biosorption and biocoagulation with *Spirogyra rhizopus*," *Dyes and Pigments*, vol. 71, no. 2, pp. 83–89, 2006.

[48] W. Cheng, S.-G. Wang, L. Lu et al., "Removal of malachite green (MG) from aqueous solutions by native and heat-treated anaerobic granular sludge," *Biochemical Engineering Journal*, vol. 39, no. 3, pp. 538–546, 2008.

[49] S. Banerjee and M. C. Chattopadhyaya, "Adsorption characteristics for the removal of a toxic dye, tartrazine from aqueous solutions by a low cost agricultural by-product," *Arabian Journal of Chemistry*, vol. 10, pp. 1629–1638, 2017.

[50] N. Nabbou, M. Belhachemi, M. Boumelik et al., "Removal of fluoride from groundwater using natural clay (kaolinite): optimization of adsorption conditions," *Comptes Rendus Chimie*, vol. 22, no. 2-3, pp. 105–112, 2019.

[51] L. B. L. Lim, N. Priyantha, D. T. B. Tennakoon, H. I. Chieng, M. K. Dahri, and M. Suklueng, "Breadnut peel as a highly effective low-cost biosorbent for methylene blue: equilibrium, thermodynamic and kinetic studies," *Arabian Journal of Chemistry*, vol. 10, pp. 3216–3228, 2017.

[52] Y. Hu, Y. Zhang, Y. Hu et al., "Application of wasted oolong tea as a biosorbent for the adsorption of methylene blue," *Journal of Chemistry*, vol. 2019, Article ID 4980965, 10 pages, 2019.

[53] E. Daneshvar, A. Vazirzadeh, A. Niazi, M. Kousha, M. Naushad, and A. Bhatnagar, "Desorption of methylene blue dye from brown macroalga: effects of operating parameters, isotherm study and kinetic modeling," *Journal of Cleaner Production*, vol. 152, pp. 443–453, 2017.

[54] Z. Liang, Z. Zhao, T. Sun, W. Shi, and F. Cui, "Enhanced adsorption of the cationic dyes in the spherical CuO/mesosilica nano composite and impact of solution chemistry," *Journal of Colloid and Interface Science*, vol. 485, pp. 192–200, 2017.

[55] P. Manoj Kumar Reddy, K. Krushnamurty, S. K. Mahammadunnisa, A. Dayamani, and Ch. Subrahmanyam, "Preparation of activated carbons from bio-waste: effect of surface functional groups on methylene blue adsorption," *International Journal of Environmental Science and Technology*, vol. 12, no. 4, pp. 1363–1372, 2015.

[56] H. Han, W. Wei, Z. Jiang, J. Lu, J. Zhu, and J. Xie, "Removal of cationic dyes from aqueous solution by adsorption onto hydrophobic/hydrophilic silica aerogel," *Colloids and Surfaces A: Physicochemical and Engineering Aspects*, vol. 509, pp. 539–549, 2016.

[57] S. I. Siddiqui, G. Rathi, and S. A. Chaudhry, "Qualitative analysis of acid washed black cumin seeds for decolorization of water through removal of highly intense dye methylene blue," *Date in Brief*, vol. 20, pp. 1044–1047, 2018.

[58] E. M. Ben'ko and V. V. Lunina, "Adsorption of methylene blue on lignocellulosic plant materials," *Russian Journal of Physical Chemistry A*, vol. 92, no. 9, pp. 1794–1798, 2018.

[59] M. Gouamid, M. R. Ouahrani, and M. B. Bensaci, "Adsorption equilibrium, kinetics and thermodynamics of methylene blue from aqueous solutions using date palm leaves," *Energy Procedia*, vol. 36, pp. 898–907, 2013.